Communication of IUGS Geological Standards

by Andrzej Wierzbowski[1], Marcin Barski[1], Angela L. Coe[2], Mark W. Hounslow[3], Bronisław A. Matyja[1], Gregory D. Price[4], Hubert Wierzbowski[5], John K. Wright[6], with contributions from Francois Atrops[7], Jacek Grabowski[5], Emanuela Mattioli[7], Nicol Morton[8], James G. Ogg[9], Federico Olóriz[10], Kevin Page[11], Horacio Parent[12], Piotr Przybylski[13], Guenter Schweigert[14], and Anna Bertha Villaseñor[15]*

The Global Stratotype Section and Point (GSSP) for the base of the Kimmeridgian Stage (Jurassic System), at Flodigarry, Staffin Bay, Isle of Skye, Scotland, UK – Supplement

[1] Faculty of Geology, University of Warsaw, Warszawa, Poland
[2] School of Environment, Earth and Ecosystem Sciences, The Open University, Milton Keynes, MK7 6AA, UK; *Corresponding author, *E-mail: angela.coe@open.ac.uk*
[3] Lancaster Environmental Centre, Lancaster University, Lancaster, LA1 4YQ, UK and Earth, Ocean and Ecological Sciences, University of Liverpool, Liverpool, L69 3GP, UK
[4] School of Geography, Earth and Environmental Sciences, University of Plymouth, Drake Circus, Plymouth, PL4 8AA, UK
[5] Polish Geological Institute–National Research Institute, Warszawa, Poland
[6] Department of Earth Sciences, Royal Holloway, Egham, TW20 0EX, UK
[7] Laboratoire de Geologie, Université de Lyon 1, F-69622 Villeurbanne, France
[8] 07200 Vogue, France
[9] Department of Earth and Atmospheric Sciences, Purdue University, Indiana, USA and State Key Laboratory of Oil and Gas Reservoir Geology and Exploitation, Institute of Sedimentary Geology, Chengdu University of Technology, Chengdu 610059, China
[10] Facultad de Ciencias, Universidad de Granada, Granada, Spain
[11] Camborne School of Mines, University of Exeter, Penryn, Cornwall, TR10 9FE, UK
[12] Universidad Nacional de Rosario, Rosario, Argentina
[13] BP America Inc. Southern Performance Unit, Houston, USA
[14] Staatliches Museum für Naturkunde, Stuttgart, Germany
[15] Departamento de Paleontologia, Instituto de Geologia, Ciudad México, Mexico

(Received: November 8, 2022; Revised accepted: November 24, 2022)

https://doi.org/10.18814/epiiugs/2022/022046

Appendix 1. Summary of the History of the Proposal, Voting and Revisions

This proposal, prepared by members of the Kimmeridgian Working Group (KWG) of the International Subcommission on Jurassic Stratigraphy led by Andrzej Wierzbowski is a summary based on a number of earlier publications, especially those of Matyja et al. (2004, 2006), and Wierzbowski A. et al. (2006, 2016, 2018), along with unpublished work. The proposal follows on from voting (from 28.04.2016 to 26.06.2016) in the KWG on the proposal that the Kimmeridgian Working Group recognizes the *Pictonia flodigarriensis* ammonite horizon as the lowest level of the Subboreal Baylei Zone in the Flodigarry section, Staffin Bay of Skye (northern Scotland) marking the Global Stratotype Section and Point for the base of the Kimmeridgian Stage. The number of votes received exceeded the quorum of 60% necessary for approval the decision at 71.8% (28 of 39 members of KWG). The results of voting were: for – 26 votes (92.86%), against – one vote (3.7 %), abstain – 1 vote (3.7%).

This is an extensively revised version of the original proposal which was first sent to the International Subcommission on Jurassic Stratigraphy (ISJS) in June 2017 and then December 2018 for feedback. Following the recommendations of the voting members of the ISJS the text has been supplemented in several ways. These include providing: (1) a sharper definition of the *flodigarriensis* horizon– which following an additional study of the ammonite faunas (Wierzbowski et al., 2018) is determined to occur over a narrow stratigraphic interval (1.60 m, spanning from 1.24 m below the base of bed 36 to 0.2 m above the top of bed 36); (2) photographs of the key ammonite taxa and the lithological succession at Flodigarry on the Isle of Skye; (3) documentation of the occurrences and ranges of all major macro- and microfossils to date in the Flodigarry section, including nannofossils and dinoflagellate cysts across the Oxfordian/Kimmeridgian boundary (Ustinova, 2018; Barski, 2018); (4) additional documentation/discussion of the global correlative value of ammonite taxa other than those which locally make up the *flodigarriensis* horizon; (5) some additional comments on the magnetostratigraphy (see Appendix 3), and isotope stratigraphy; (6) clarification of the text, figures

and interpretation of the raw data; (7) corrections to the magnetostratigraphy, and (8) discussion of the sequence stratigraphy and climatic conditions; (9) comments on GTPS 2020.

On May 16th 2019, based on this revised proposal, ISJS voted by an overwhelming majority that 'the GSSP for the base Kimmeridgian should be placed 1.25 m below the top of Bed 35 of the Staffin Shale Formation at Flodigarry, Staffin Bay, Isle of Skye, Scotland'. In the voting quorum was exceeded at 95% (21 of the 22 voting members); of those voting 20 were in favour (95%) and one abstained (5%). The International Commission on Stratigraphy voted unanimously in favour of the proposal on 24th January 2021 and this was ratified by the International Union of Geological Sciences on the 14th February 2021.

APPENDIX 2 – Ammonite, Dinocyst and Nannofossil Occurrences

1. Ammonite Occurrences from Flodigarry

List of the ammonites and their stratigraphic position from the base of the section upwards. The list also provides notes on which ammonite samples were used to obtain matrix for dinoflagellate studies. The section and previous studies are described in Wierzbowski A. et al. (2006), minor modifications based on further work have been made to the thicknesses given here. The ammonites are housed in the collections of the University Museum, Oxford, UK (collection ST600 to ST926; Matyja et al., 2006), and the Geological Faculty Museum of Warsaw University, Poland (collection MWG UW ZI/94/01 to UW ZI/94/55; Wierzbowski A. et al., 2018).

Bed 33 (the uppermost 9.5 m of this bed were studied):

14.72 m below base of bed 36 – *Ringsteadia caledonica* Sykes et Callomon;
13.85 m below base of bed 36 – *Microbiplices* ex gr. *procedens* (Oppen.) - *guebhardi* (Oppen.);
13.85 m below base of bed 36 – *Ringsteadia brandesi* Salfeld;
13.85 m below base of bed 36 – *Amoeboceras regulare* Spath;
9.93 m below base of bed 36 – *Amoeboceras regulare* Spath;
7.5 m below base of bed 36 – *Ringsteadia* ex gr. *pseudoyo* Salfeld;
7.5 m below base of bed 36 – *Amoeboceras marstonense* Spath;
7.28 m below base of bed 36 – *Microbiplices anglicus* Arkell;
7.28 m below base of bed 36 – *Microbiplices microbiplex* (Quenstedt);
6.43 m below base of bed 36 – *Ringsteadia* cf. *pseudocordata* (Blake et Hudleston);
6.34 m below base of bed 36 – *Ringsteadia* cf. *pseudocordata* (Blake et Hudleston);
6.34 m below base of bed 36 – *Amoeboceras rosenkrantzi* Spath;
6.34 m below base of bed 36 – *Amoeboceras leucum* Spath;
6.34 below base of bed 36 – *Amoeboceras marstonense* Spath;

Bed 34 (thickness 0.20 m): – *Amoeboceras* cf. *leucum* Spath;

Bed 35 (thickness 6.0 m):

– lowermost part - from its base up to 0.5 m above:
Ringsteadia pseudocordata (Blake et Hudleston) – 3 specimens;
Microbiplices microbiplex/ cf. *microbiplex* (Quenstedt) – 3 specimens;
Microbiplices cf. *anglicus* Arkell – 1 specimen;
Amoeboceras rosenkrantzi Spath – 3 specimens;
Amoeboceras cf. *rosenkrantzi* Spath – 3 specimens;
Amoeboceras marstonense Spath – 1 specimen;

– upper and middle parts:

2.34 m below base of bed 36 – *Ringsteadia* sp. (densely ribbed inner whorls);
2.34 m below base of bed 36 – *Microbiplices anglicus* Arkell;
2.34 m below base of bed 36 – *Microbiplices microbiplex* (Quenstedt);
about 1.5–2 m below base of bed 36 – *Amoeboceras* cf. *rosenkrantzi* Spath;
1.9 m below base of bed 36 – *Ringsteadia* cf. *frequens* Salfeld;
1.8 m below base of bed 36 – *Ringsteadia evoluta* Spath; Matrix from this sample was used for dinoflagellates (sample 1 of Barski (2018))
1.65 m below base of bed 36 – *Microbiplices/Prorasenia* transitional form;
1.65 m below base of bed 36 – *Ringsteadia evoluta* Spath;
1.5 m below base of bed 36 – *Ringsteadia* cf. *evoluta* Salfeld;
1.44 m, and 1.45 m below base of bed 36 – *Amoeboceras rosenkrantzi* Spath – 2 specimens;
1.44 m below base of bed 36 – *Amoeboceras* cf. *schulginae* Mesezhnikov; Matrix from this sample was used for dinoflagellates (sample 2 of Barski (2018)).
1.4 m below base of bed 36 – *Microbiplices/Prorasenia* transitional form – two specimens;
1.4 m below base of bed 36 – *Ringsteadia evoluta* Salfeld;
1.26 m below base of bed 36 – *Ringsteadia frequens* Salfeld;
1.24 m below base of bed 36 – *Pictonia* (*Triozites*) cf. *seminudata* Buckman; Matrix from this sample was used for dinoflagellates (sample 3 of Barski (2018))
1.17 m below base of bed 36 – *Plasmatites praebauhini* (Salfeld) – *Amoeboceras rosenkrantzi* Spath trans.form;
1.17 m below base of bed 36 – *Amoeboceras rosenkrantzi* Spath;
1.17 m below base of bed 36 – *Plasmatites praebauhini* (Salfeld);
1.10 m below base of bed 36 – *Microbiplices/Prorasenia* transitional form;
1.08 m below base of bed 36 – *Plasmatites* sp. and *Amoeboceras* (? *rosenkrantzi*) – 2 specimens;
1.08 m below base of bed 36 – *Pictonia flodigarriensis* Matyja et al.; Matrix from this sample was used for dinoflagellates (sample 4 of Barski (2018)).
1.08 m below base of bed 36 – *Prorasenia bowerbanki* Spath;
1.07 m below base of bed 36 – *Plasmatites praebauhini* (Salfeld);
1.04 m below base of bed 36 – *Amoeboceras schulginae* Mesezhnikov;
0.61 m below base of bed 36 – *Amoeboceras schulginae* Mesezhnikov;
0.60 m below base of bed 36 – *Plasmatites* aff. *bauhini* (Oppel);
0.60 m below base of bed 36 – *Prorasenia bowerbanki* Spath; Matrix from this sample was used for dinoflagellates (sample 5 of Barski (2018)).
0.56 m below base of bed 36 – *Plasmatites praebauhini* (Salfeld) – *Amoeboceras rosenkranzti* Spath trans. form;
0.54 m below base of bed 36 – *Microbiplices/Prorasenia* transitional form;
0.52 m below base of bed 36 – *Pictonia flodigarriensis* Matyja et al.;
0.52 m below base of bed 36 – *Pictonia* ex gr. *flodigarriensis* Matyja et al. – *densicostata* Buckman – 2 specimens;
0.45 m below base of bed 36 – *Pictonia* (*Triozites*) cf. *seminudata* Buckman;
0.45 below base of bed 36 – *Amoeboceras* cf. *rosenkrantzi* Spath;

039 m below base of bed 36 – *Pictonia flodigarriensis* Matyja et al.;
0.39 m below base of bed 36 – *Prorasenia bowerbanki* Spath;
0.3 m below base of bed 36 – *Plasmatites* sp.;
0.3 m below base of bed 36 – *Pictonia* sp.;
0.17 m below base of bed 36 – *Amoeboceras schulginae* Mesezhnikov;

Bed 36 (thickness 0.07–0.35 m);

Bed 37 (thickness 4.17 m):

– lower part:

017 m above top of bed 36 – *Amoeboceras schulginae* Mesezhnikov;
0.2 m above top of bed 36 – *Pictonia flodigarriensis* Matyja et al.;
0.2 m above top of bed 36 – *Prorasenia bowerbanki* Spath;
0.2 m above top of bed 36 – *Amoeboceras rosenkrantzi* Spath;
(0–0.5 m above the base of bed 36 dinoflagellate sample 6 of Barski (2018))
0.88 m above top of bed 36 – *Plasmatites* cf. *bauhini* (Oppel);
0.9 m above top of bed 36 – *Pictonia densicostata* Buckman;
1.0 m above top of bed 36 – *Pictonia densicostata* Buckman;

– upper part:

1.4 m below base of bed 38 – *Plasmatites bauhini* (Oppel);
1.4 m below base of bed 38 – *Plasmatites lineatum* (Quenstedt);
1.4 m below base of bed 38 – *Plasmatites praebauhini* (Salfeld);
1.3 m below base of bed 38 – *Plasmatites bauhini* (Oppel);
1.3 m below base of bed 38 – *Plasmatites lineatum* (Quenstedt);
1.3 m below base of bed 38 – *Plasmatites praebauhini* (Salfeld);
0.97 m below base of bed 38 – *Plasmatites lineatum* (Quenstedt);
0.50 m below base of bed 38 – *Plasmatites bauhini* (Oppel);
0.50 m below base of bed 38 – *Pictonia densicostata* Buckman;
0.30 m below base of bed 38 – *Pictonia densicostata* Buckman;
0.20 m below base of bed 38 – *Plasmatites bauhini* (Oppel);

Specimens from upper part of bed 37 not precisely located: *Plasmatites praebauhini* (Salfeld); *Plasmatites* spp., *Prorasenia* sp., *Pictonia* cf. *densicostata* Buckman.

Bed 38 (thickness 0.28 m):

Pictonia deniscostata Buckman – numerous specimens;
Prorasenia cf. *bowerbanki* Spath;
Plasmatites bauhini (Oppel);
Plasmatites praebauhini (Salfeld);

Bed 39 (thickness 1.92 m):

Amoeboceras aff. *schulginae* Mesezhnikov – 7.96 m below bed 44 – 3 specimens;
Pictonia baylei Salfeld/*P. normandiana* Tornquist – 6.6 m below bed 44;

Bed 40 (thickness 0.15–0.45 m);

Bed 41 (thickness 1.52 m):

Plasmatites bauhini (Oppel) – 5.9 m below base of bed 44;
Pictonia baylei Salfeld / *normandiana* (Tornquist) – 5.9 m below base of bed 44;
Pictonia normandiana Tornquist – 5.8 m below base of bed 44;
Pictonia baylei Salfeld/*P. normandiana* Tornquist – 5.7 m below base of bed 44;
Plasmatites lineatum (Quenstedt) – 5.7 m below base of bed 44;
Plasmatites bauhini (Oppel) – 5.7 m below base of bed 44;
Prorasenia hardyi Spath – 5.7 m below base of bed 44;
Plasmatites lineatum (Quenstedt) – 5.66 m below base of bed 44;
Plasmatites bauhini (Oppel) – 5.65 m below base of bed 44;
Plasmatites bauhini (Oppel) – 5.5 m below base of bed 44;
Pictonia baylei Salfeld /*normandiana* (Tornquist) – 5.4 m below base of bed 44;
Amoebites bayi Birkelund et Callomon – 4.99 m below base of bed 44;
Amoebites cricki (Salfeld) – 4.99 m below base of bed 44;
Amoebites bayi – Plasmatites bauhini trans. form – 4.99 m below base of bed 44;

Bed 42 (thickness 0.40 m):

Amoebites bayi – Plasmatites bauhini trans. form – 4.79 m below base of bed 44;
Amoebites bayi Birkelund et Callomon – 4.79 m below base of bed 44;
Amoebites cricki (Salfield) – 4.79 m below base of bed 44;
Pictonia sp. – not precisely located;
Not precisely located sample 7 used for dinoflagellates (see Barski (2018)).

Bed 43 ((thickness 4.39 m):

Pictonia baylei Salfeld/*P. normandiana* Tornquist – 4.1 m below base of bed 44;
Amoebites cricki (Salfield) – 4.1 m below base of bed 44;
Amoebites bayi Birkelund et Callomon – 4.0 m below base of bed 44;
Prorasenia hardyi Spath – 3.9 m below base of bed 44;
Rasenia inconstans Spath – 2.3 m and 0.6 m below base of bed 44 (2 specimens);

Bed 44 (thickness 0.17 m):

Rasenia inconstans Spath;

Bed 45 (thickness 1.6 m of interval studied):

Amoebites subkitchini Spath – 1.37 m above top of bed 44;
Rasenia sp. – 1.6 m above top of bed 44.

2. Dinoflagellate cyst species from Flodigarry

For further information on the stratigraphic position of the samples see Barski (2018) and figure 7. The notes above on the ammonites (Appendix 2.1) indicate where the matrix used for the dinoflagellate samples were taken.

Gonyaulacysta jurassica jurassica (Deflandre, 1938)
Gonyaulacysta dentata (Raynaud, 1978)
Leptodinium subtile Klement, 1960
Rhynchodiniopsis cladophora (Deflandre, 1938)
Sirmiodinium grossi Albert, 1961
Scriniodinium crystallinum (Deflendre, 1938)
Scriniodinium dictyotum papillatum (Gitmez, 1970)
Scriniodinium dictyotum osmingtonense Gitmez, 1970
Scriniodinium inritibile Riley, 1980
Endoscrinium galeritum (Deflandre, 1938)
Stephanelytron redcliffense Sarjeant, 1961
Senoniasphaera jurassica (Gitmez and Sarjeant, 1972)
S. aff. *jurassica*
Perisseiasphaeridium pannosum Davey and Williams, 1966
Emmetrocysta sarjeanti Gitmez, 1970
Hystrichosphaerina ? *orbifera* (Klement, 1960)
Ellipsoidictyum cinctum Klement, 1960
Prolixosphaeridium anasillum Erkman and Sarjeant, 1980
Atopodinium haromense Thomas and Cox, 1988
Adnatosphaeridium caulleryi (Deflandre, 1939)
Ambonosphaera ? *staffinensis* (Gitmez, 1970)
Endoscrinium luridum (Deflandre, 1939)

Cribperidinium globatum (Gitmez and Sarjeant, 1972)
Glossodinium dimorphum Ioannides et al., 1977
Pareodinia ceratophora Deflandre, 1947
Systematophora areolata Klement, 1960
Tubotuberella apatela (Cookson and Eisenack, 1960)
Valensiella ovulum (Deflandre, 1947)
Dingodinium jurassicum Cookson and Eisenack, 1958
Dingodinium tuberosum Gitmez, 1970.

3. Nannofossil Species from Flodigarry

For further information on the samples and their stratigraphic positions see Ustinova (2018). The only stratigraphically significant nannofossil found to date is *O. decussatus* from sample 3 which was taken in bed 35 at 2.34 m below base of bed 36.

Crepidolithus perforata (Medd, 1979) Grün and Zweili, 1980
Cyclagelosphaera margerelii Noël, 1965
C. lacuna (Grün and Zweili, 1980) Cooper, 1987. In Nannotax, this is considered as a synonym of *C. tubulata.*
Ethmorhabdus gallicus Noël, 1965
Hexapodorhabdus cuvilleri Noël, 1965
Octopodorhabdus decussatus (Manivit, 1961) Rood et al., 1971
Podorhabdus grassei Noël, 1965
Retecapsa escaigii (Noël, 1965) Young and Bown, 2014
Retecapsa cf. *R. incompta* Bown, 1987. Range: Upper Toarcian – Middle? Oxfordian (Bown and Cooper, 1998). The species from the Flodigarry section has a more delicate and less distinct central structure.
R. octofenestrata (Bralower in Bralower et al.,1989), Bown *in* Bown and Cooper, 1998
Retecapsa schizobrachiata (Gartner, 1968) Grün in Grün and Allemann, 1975.
Sollasites lowei (Bukry, 1969) Rood et al., 1971
Stephanolithion bigotii bigotii Deflandre, 1939
Triscutum? sp., Dockerill, 1987
Watznaueria barnesiae (Black, 1959) Perch-Nielsen, 1968
W. britannica (Stradner, 1963) Reinhardt, 1964
W. fossacincta (Black, 1971a) Bown in Bown and Cooper, 1989a
Watznaueria manivitiae Bukry, 1973d
Zeugrhabdotus erectus (Deflandre in Deflandre and Fert, 1954), Reinhardt, 1965
Z. fissus Grün and Zweili, 1980.

APPENDIX 3 – Magnetostratigraphic Data

Table S1. Summary of palaeomagnetic data for each specimen from the Flodigarry Section

Sample[a]	Sample position	Bedding strike		ChRM		Class[c]	GC pole[d]		VGP Lat[e]		FT[f]	Mean[g]	Pol.[h]
		Strike	Dip	Ds[b]	Is[b]		Ds[b]	Is[b]	S	T			
mwh11a		158	70			T	47	–25		–74		yes	R??
mwh11b	6.00 m above top of bed 44	158	70			T	258	–36		–43		yes	R???
mwh11c		158	70			T	214	–3		–26			R??
STF745F	5.37 m above top of bed 44	158	69	313	–39	Sx	0	0	12	0			?
STF745E	5.25 m above top of bed 44	158	69	346	9	S	93	56	54			yes	N??
STF745D	4.27 m above top of bed 44	158	69			T	73	18		45			N??
STF745C	3.15 m above top of bed 44	158	69	294	–22	Sx			1				R??
STF745B	2.08 m above top of bed 44	158	69			T	209	–34		9			R??
STF745A	1.10 m above top of bed 44	158	69			T	280	41		–67		yes	R??
STF744B	0.03 m below top of bed 44	162	70	162	–6	Sx			–49				R??
mwh1a		158	78			T	139	8		–70	x	yes	R??
mwh1b	Bed 44	158	78			T	77	8		–56	x	yes	R??
mwh1d		158	78			T	321	–62		–71	x	yes	R??
STF744A	0.03 m above base of bed 44	162	70	313	–48	Sx			7				R??
mwh2a		158	78			T	269	7		–81	x	yes	R???
mwh2b	2.30 m below base of bed 44	158	78			T	177	9		–48	x	yes	R?
mwh2d		158	78			T	45	–23		–71	x	yes	R??
STF743B	1.73 m below base of bed 44	177	84			T	205	–69		52			N??
STF743A	1.20 m above base of bed 43	177	84			T	234	–60		42			N??
STF742	0.08 m above base of bed 42	177	84	176	–48	S	192	46	–72	–89	x	yes	R
STF741	0.85 m above base of bed 41	177	84	203	–41	S			–83		x	yes	R
STF240A	0.20 m above base of bed 40	159	52	244	–28	S	192	53	–45	–84	x	yes	R
STF740	Middle of bed 40	177	84	233	–47	S			–58		x	yes	R
STF739	0.51 m below base of bed 40	177	84	187	–61	S	201	32	–73	–78	x	yes	R?
STF238C	0.35 m above base of bed 38	159	52	244	–21	S	15	–58	–43	–81	x	yes	R

Table S1. (continued)

Sample[a]	Sample position	Bedding strike		ChRM		Class[c]	GC pole[d]		VGP Lat[e]		FT[f]	Mean[g]	Pol.[h]
		Strike	Dip	Ds[b]	Is[b]		Ds[b]	Is[b]	S	T			
mwh14a	Base of bed 38	148	76			T	273	–18		–63		yes	R??
mwh14b		148	76			T	269	–7		–68		yes	R??
mwh14i		148	76			T	293	1		–84		yes	R???
mwh14j		148	76			T	285	13		–80		yes	R??
STF238B	0.09 m above base of bed 38	159	71	253	45	Sx			–14				R??
STF238A	0.08 m above base of bed 38	163	63	8	47	S	161	35	82		x	yes	N?
STF738	0.05 m above base of bed 38	177	84			T	36	14		12			N??
STF737	0.23 m below base of bed 38	177	84			T	301	–46		–69		yes	R?
STF237D	1.10 m below base of bed 38	159	52	166	16	Sx			–44				R??
STF237E	1.25 m below base of bed 38	159	52			T	235	–40		25			N??
STF237C	1.6 m below base of bed 38	159	52	208	–11	S			–66		x	yes	R?
mwh15a	2.00 m below base of bed 38	148	76			T	128	21		89		yes	N??
mwh15b		148	76	61	48	S	296	0	51	82	x	yes	N?
STF237B	1.4 m above base of bed 37	159	52			T	24	68		–52		yes	R??
mwh16a	3.70 m below base of bed 38	144	75			T	215	–5		–24			R???
mwh16B		144	75			T	15	–4		–35		yes	R??
mwh16c		144	75			T	12	26		16			R??
STF237A	0.39 m above base of bed 37	159	52			T	185	46		–89		yes	R?
jw19	Top surface of bed 36	168	65			T	260	8		–87		yes	R??
STF236B	0.1 m above base of bed 36	159	52			T	127	41		–74		yes	R?
STF236A	0.07 m above base of bed 36	159	52	244	8	Sx			–35				R??
jw2.1	0.08 m below base bed 36	168	65	174	–41	S	62	–65	–78		x	yes	R?
jw3.3	0.28 m below base bed 36	168	65			T	196	37		–89		yes	R?
jw4.1	0.51 m below base of bed 36	168	65			T	2	–53		–79		yes	R??
jw7.1	0.8 m below base bed 36	168	65	216	–67	S	209	28	–60		x	yes	R??
jw8.3	1.05 m below base bed 36	168	65			T	267	2		–86		yes	R??
jw9.1	1.28 m below base bed 36	168	65	186	–32	S	249	39	–76		x	yes	R?
STF235A	1.38 m below base of bed 36	167	43	54	29	S			53		x	yes	N??
STF235B	1.38 m below base of bed 36	167	43			T	318	–30		–88		yes	R??
jw18.1	1.48 m below base of bed 36	168	65	332	50	S	94	24	63		x	yes	N?
jw10.3	1.5 m below base of bed 36	168	65	357	41	S			80		x	yes	N?
jw20.1	1.83 m below base of bed 36	168	65	51	57	S	203	21	51		x	yes	N?
jw11.2	1.85 m below base of bed 36	168	65	28	60	S	300	–8	69		x	yes	N?
mwh5a	2.00 m below base of bed 36	168	68			x							?
mwh5b		168	68			x							?
mwh5c		168	68	2	57	S	255	–9	74	54	x	yes	N
mwh5d		168	68			T	296	–5		86		yes	N???
mwh5e		168	68			T	152	0		51		yes	N???
jw12.1	2.35 m below base of bed 36	168	65	354	46	S	99	17	80		x	yes	N
STF235C	2.40 m below base of bed 36	167	43			T	295	–69		–63		yes	R??
jw13.2	2.60 m below base of bed 36	168	65			T	3	–17		–63		yes	R?
jw14.3	3.05 m below base of bed 36	168	65			T	47	–29		–88		yes	R???
jw15.1	3.50 m below base of bed 36	168	65			T	150	46		–80		yes	R?
jw16.1	3.90 m below base of bed 36	168	65			T	257	19		–85		yes	R??
jw17.3	4.20 m below base of bed 36	168	65			T	195	–32		12		yes	R???
STF235D	1.65 m above base of bed 35	167	43	14	25	S			76		x	yes	N??

Table S1. (continued)

Sample[a]	Sample position	Bedding strike		ChRM		Class[c]	GC pole[d]		VGP Lat[e]		FT[f]	Mean[g]	Pol.[h]
		Strike	Dip	Ds[b]	Is[b]		Ds[b]	Is[b]	S	T			
STF235F	0.01 cm above base of bed 35	167	43	58	56	S			54		x	yes	N??
STF235E	0.6 m below base of bed 35	167	43	201	–34	S			–81		x	yes	R
STF234A	Middle of bed 34	148	31			T	129	3		–73		yes	R??
STF233A	0.30 m below base of bed 34	148	31			T	62	–13		–67		yes	R??
mwh6a		158	60			T	30	12		–9			R??
mwh6b	8.00 m below base of bed 36	158	60			T	149	5		–59		yes	R???
mwh6c		158	60			T	58	24		–27			R??
STF233B	3.45 m below base of bed 34	148	31			T	210	8		–44		yes	R??
mwh8a		158	70			x							?
mwh8b	12.5 m below base of bed 36	158	70			x							?
mwh8c		158	70	199	–47	S			–87		x	yes	R
mwh8d		158	70	194	–30	S	105	2	–79	–87		yes	R
mwh10a		153	73			T	81	1		–66	x	yes	R
mwh10b	15.0 m below base of bed 36	153	73			T	285	–7		–82	x	yes	R??
mwh10d		153	73			T	97	7		–75	x	yes	R??
mwh10e		153	73			T	305	–33		–78		yes	R
STF233C	6.32 m below base of bed 34	148	31	51	63	S	67	–23	57	81	x	yes	N??

[a]Sample codes are STF for those collected and measured by Jim Ogg and Angela Coe, mwh and jw are those collected by John Wright and analysed by Mark Hounslow. Samples marked mwh, jw and STF7xx were collected from Point 7, STF2xx from Point 2. The STF and mwh data is also detailed in Wierzbowski A. et al. (2006) and Przybylski et al. (2010b) and the JW data is in Wierzbowski A. et al. (2016).
[b]Ds and Is are declination and inclination in stratigraphic coordinates.
[c]Class is the demagnetisation behaviour class, with S indicating a PCA line fit, Sx a poor PCA line fit, T great circle type behaviour without recovery of PCA line fit.
[d]GC pole is the pole to the fitted great circle (see Hounslow et al., 2008).
[e]VGP Lat = virtual geomagnetic pole latitude, with values for S-class data (S) and T-class data. VGP latitude >0 is nominally normal polarity and <0 nominally reverse polarity.
[f]FT indicates if the data was used in the fold test.
[g]Mean = if data was used in the mean direction determinations in Table S2.
[h]Pol = polarity rating score (see Hounslow et al., 2008 and Przybylski et al., 2010b), such that R = good reverse, N = good normal and ? = uncertain, more question marks indicates greater uncertainty in polarity determination.

Table S2. Mean palaeomagnetic directions for the section

Type[a]	Mean Dec/Inc (°)	α95 (°)[b]	$N_T/N_l/N_p$[c]	Reversal Test [γ_o;γ_c] (°)[d]	VGP Pole Long./Lat. (°)[e]	D_p/D_m (°)
Fish-All	23.6/48.5	8.4	64/27/0	Rc [7.8;17]	133.4/57.4	7.3/11.0
Fish-R	203.0/-45.0	11.9	64/15/0	-	-	-
Fish-N	24.5/52.7	12.7	64/12/0	-	-	-
GC-All	15.6/48.2	5.5	88/27/30	Rc [11.6;16.6]	146.2/59.6	4.7/7.2
GC-R	191.8/-45.6	8.4	88/15/27	-	-	-
GC-N	25.3/53.3	11.0	88/12/3	-	-	-

[a]Type: Fisher = conventional Fisher mean, GC = combined GC mean (McFadden and McElhinny, 1988), 'All', 'R' and 'N' indicate sets of all, reverse and normal polarity samples.
[b]α95 = Fisher 95% cone of confidence.
[c]N_T = Total specimens measured (for Fisher type data, number of samples), N_l = Number of specimens with line-fits, N_p = Number of specimens with great circle fits.
[d]For the reversal test (McFadden and McElhinny, 1990), γ_o = observed angle; γ_c = critical angle at 95% confidence.
[e]Virtual geomagnetic pole (VGP) is the normal pole. Means determined with PMagTool (Hounslow, 2006).

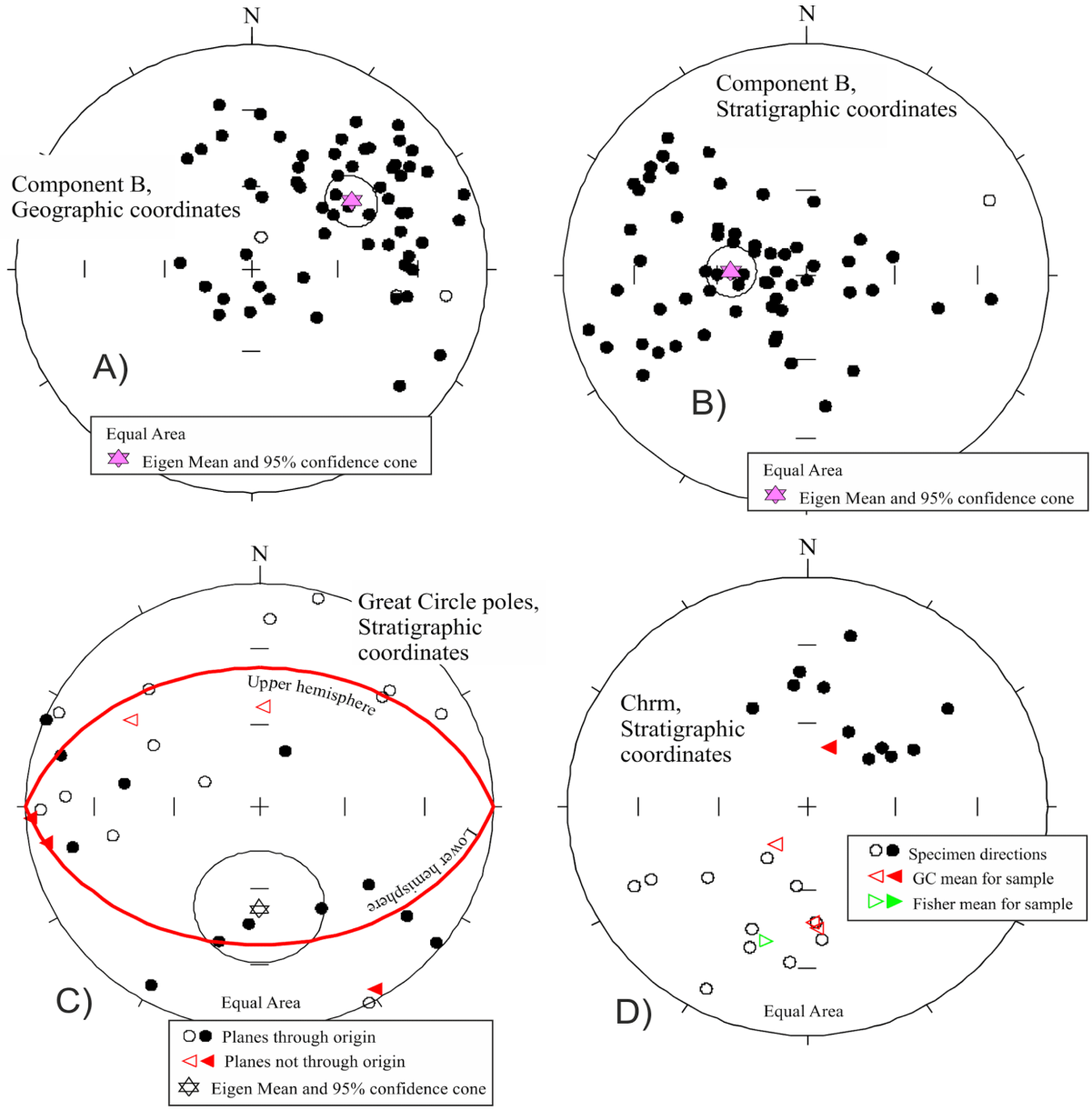

Figure S1. Directional information for magnetisation components extracted. A) and B) show all the specimen component B directions (described in Wierzbowski A. et al., 2006). The origin of the B component is not clear but may be associated with either a Brunhes age component acquired in the pre-slip position of the sections, or a composite Brunhes- Jurassic direction. C) Great circle plane information from the suitable T-class specimens (Table S1). In such a dataset the poles are spread on a girdle, with the mean axis through the girdle (shown as eigen mean and confidence interval) representing an approximation of the unresolved direction (see Hounslow et al., 2008; Hounslow et al., 2017 for further explanation). D) Characteristic remanence (ChRM) directions from the section, showing single specimens from samples, and sample means using either the combined great circle (GC) method of McElhinny and McFadden (1988) or the Fisher Mean. Mean directions and plots used PmagTool (Hounslow, 2006).

Additional References

Hounslow, M.W., Peters, C., Mørk, A., Weitschat, W., and Vigran, J.O., 2008, Biomagnetostratigraphy of the Vikinghøgda Formation, Svalbard (Arctic Norway), and the geomagnetic polarity timescale for the Lower Triassic Magnetostratigraphy. GSA Bulletin, v.120, pp. 1305–1325. doi:10.1130/B26103.1

Hounslow, M.W., White, H.E., Drake, N.A., Salem, M.J., El-Hawat, A., McLaren, S.J., Karloukovski V., Noble, S.R., and Hlal, O., 2017, Miocene humid intervals and establishment of drainage networks by 23 Ma in the central Sahara, southern Libya. Gondwana Research, v. 45, pp. 118–137. doi:10.1016/j.gr.2016.11.008

Hounslow, M.W., 2006, PMagTools version 4.2, a tool for analysis of 2-D and 3-D directional data. doi:10.13140/RG.2.2.19872.58880.

McFadden, P.L., and McElhinny, M.W., 1988, The combined analysis of remagnetisation circles and direct observations in paleomagnetism. Earth and Planetary Science Letters, v. 87, pp.161–172. doi:10.1016/0012-821X(88)90072-6

McFadden, P.L., and McElhinny, M.W., 1990, Classification of the reversal test in paleomagnetism. Geophysical Journal International, v. 103, pp. 725–729. doi:10.1111/j.1365-246X.1990.tb05683.x